ARTICLE IN PRESS

Available online at www.sciencedirect.com

SCIENCE DIRECT®

Thin Solid Films xx (2004) xxx–xxx

thin solid films

www.elsevier.com/locate/tsf

Epitaxial growth of ruthenium dioxide films by chemical vapor deposition and its comparison with similarly grown chromium dioxide films

G.X. Miao[a,b,*], A. Gupta[a], Gang Xiao[b], A. Anguelouch[c]

[a]*Center for Materials for Information Technology, University of Alabama, Tuscaloosa, Alabama 35487, USA*
[b]*Physics Department, Brown University, Providence, Rhode Island 02912, USA*
[c]*Physics and Astronomy Department, Johns Hopkins University, Baltimore, Maryland 21218, USA*

Received 11 June 2004; received in revised form 11 October 2004; accepted 25 October 2004

Abstract

Epitaxial ruthenium oxide (RuO_2) thin films have been grown on (100) TiO_2 substrates by chemical vapor deposition at temperatures as low as 300 °C using tris(2,2,6,6-tetramethyl-3,5-heptanedionato)ruthenium [$Ru(TMHD)_3$] as a precursor with oxygen carrier gas. These films exhibit low resistivity, with room-temperature values as low as ~40 μΩ cm. The surface morphology, epitaxial strain and resistivity as a function of film thickness have been compared with those of similarly deposited epitaxial CrO_2 films on TiO_2. The temperature dependence of the resistivity for both set of films can be fit well using a combination of the Bloch-Gruneisen formula for electron–phonon scattering and additional scattering terms, including magnon scattering in the case of CrO_2.

PACS: 68.55; 73.61; 75.70; 68.60.B
Keywords: Electrical properties and measurements; Magnetic properties and measurements; Organometallic vapor deposition; Structural properties

1. Introduction

Ruthenium dioxide (RuO_2) exhibits a rare combination of material properties; including a relatively low resistivity (~35 μΩ cm at room temperature), good thermal stability and high resistance to chemical corrosion [1]. These desirable characteristics have attracted attention for its application in diverse fields both in the electronics and chemical industry. In the area of microelectronics, RuO_2 has been proposed for use as an interdiffusion barrier and also as a precision resistor element [2–4]. Recent studies have also demonstrated its utility as a contact electrode material in ferroelectric random access memory devices that offers superior polarization fatigue properties with very low leakage current [5–7].

Bulk RuO_2 has a tetragonal structure (a=b=0.4499 nm, c=0.3107 nm), and is closely lattice matched with isostructural rutile oxides, such as TiO_2 (a=b=0.4594 nm, c=0.2958 nm) and CrO_2 (a=b=0.4421 nm, c=0.2916 nm). While TiO_2 is an insulating oxide, CrO_2 is a ferromagnetic half-metal in which the carriers are completely spin polarized [8]. In the past, our group and others have reported on the epitaxial growth of CrO_2 thin films on TiO_2 substrates using chemical vapor deposition (CVD) under atmospheric conditions and have studied its electrical and magnetic properties [9–12]. In this paper, we report on the low-temperature epitaxial growth of RuO_2 films on (100)-oriented TiO_2 substrate using atmospheric pressure CVD and compare its structural and electrical properties with similarly grown CrO_2 films. In recent years, there have been a number of reports on the CVD growth of RuO_2 films using various metal-organic precursors [13]. However, most of the effort has been

* Corresponding author. Center for Materials for Information Technology, University of Alabama, Tuscaloosa, Alabama 35487, USA. Tel.: +1 2053484880; fax: +1 2053482346.
E-mail address: gmiao@mint.ua.edu (G.X. Miao).

0040-6090/$ - see front matter © 2004 Elsevier B.V. All rights reserved.
doi:10.1016/j.tsf.2004.10.032

directed towards deposition of polycrystalline thin films on substrates relevant for present-day electronic applications, such as Si and SiO_2. There has been limited work on the epitaxial deposition of RuO_2 films on lattice-matched substrates, such as TiO_2, MgO and Al_2O_3, and for the most part the growth in these cases have required relatively high temperatures (≥500 °C) [14–16].

Motivated by the giant magnetoresistance (GMR) effect in traditional ferromagnet/metal/ferromagnet multilayers, we have been interested in the possibility of fabricating heteroepitaxial oxide structures, such as $CrO_2/RuO_2/CrO_2$, and investigating their magnetoresistive (MR) properties. Band structure calculations suggest that such heterostructures can possibly exhibit significantly enhanced MR resulting from transport of completely spin-polarized carriers from the ferromagnetic CrO_2 layers across the conducting, but non-magnetic, RuO_2 spacer layer and interfaces [17]. The fabrication of such multilayer structures has, however, proven to be a challenging task, primarily because of the process limitations. Because of the metastabilty of CrO_2, it is difficult to synthesize at normal atmosphere, and there is only a narrow temperature window around 400 °C that single-phase epitaxial films of this material can be grown using CVD. In addition, CrO_2 is unstable at much higher temperatures, as it decomposes to form Cr_2O_3. It is thus necessary to identify an adequate precursor(s) that will enable growth of RuO_2 under process conditions compatible with the growth and stability of CrO_2. By using tris(2,2,6,6-tetramethyl-3,5-heptanedionato)ruthenium [$Ru(TMHD)_3$] as a CVD precursor [18], we have achieved growth of high-quality epitaxial RuO_2 films at temperatures as low as 300 °C. The ability to deposit RuO_2 films under conditions that are well-suited with the growth of CrO_2 now offers the possibility of fabricating RuO_2/CrO_2 heterostructures and investigating their MR properties and magnetic anisotropy.

2. Experimental details

Epitaxial RuO_2 films are grown on (100)-oriented TiO_2 substrates by the thermal decomposition of $Ru(TMHD)_3$ precursor (99%, STREM Chemicals) under atmospheric conditions in a 1-in. diameter quartz CVD reactor tube placed inside a two-zone furnace. The precursor material is loaded inside a small quartz boat in the source zone, while the substrates are placed in the higher temperature reaction zone on a specially designed susceptor with independent heating capability. Prior to placement in the susceptor, the TiO_2 substrates are ultrasonically cleaned with acetone and isopropyl alcohol and then dipped in a dilute HF bath for a few minutes. They are subsequently rinsed in de-ionized water and blown dry. Oxygen is used as a carrier gas for the precursor with typical flow rates of about 50 cm^3/min. The use of a susceptor that has independent temperature control provides added flexibility for optimizing the process conditions for film growth and uniformity by controlling the decomposition zone of the organometallic precursor in the proximity of the substrate. We have achieved epitaxial growth of RuO_2 films, with good uniformity, at substrate temperatures of 300–400 °C, while the source temperature maintained at 130 °C. The film roughness has been observed to increase with growth temperature, and all the reported results in this paper are for RuO_2 films grown at 300 °C, unless mentioned otherwise. The same setup has been utilized for the epitaxial growth of CrO_2 films on (100) TiO_2 substrates using CrO_3 as a precursor [9]. For optimal growth, the precursor and substrate temperatures in this case are maintained at 260 and 400 °C, respectively. The film surface morphology is characterized on a Digital Instruments AFM with Veeco Nanoscope III SPM controller and standard TappingMode with Si cantilever tips oscillating at about 200 kHz are used for all the measurements. The structural characterization is performed in a Philips X'Pert XRD system operating with Cu Kα1 and Kα2 radiation. Film resistivity is measured with four-probe method on Hall bars (8:1 aspect ratio) patterned along *b* or *c* directions by ion-milling.

3. Results and discussion

Although RuO_2 and CrO_2 possess the same rutile structure, there are significant differences in the lattice-strain properties of the respective films deposited on (100) TiO_2 substrate that influence their growth characteristics. As compared to the TiO_2 lattice, bulk RuO_2 has a lattice mismatch of about −2.1% and +5.0% in the [010] and [001] directions, respectively. The equivalent mismatch numbers for CrO_2 are −3.8% and −1.4%. Thus, RuO_2 thin films experience a combination of tensile and compressive strain in the two in-plane directions, with more influence of the latter directed along [001]. In contrast, the CrO_2 films grow with tensile strain in both directions, with [001] being the direction of lower strain. Interestingly, the differences in the strain characteristics of the two films are reflected in their growth morphology, as seen in the atomic force microscopy (AFM) images in Fig. 1. For the growth of both materials, one observes the formation of rectangular platelets, with the orientation of the long axis of the platelets being along the direction of lower strain. Thus, in the case of RuO_2, the grains nucleate and grow preferentially along the [001] direction leading to formation of platelets oriented in this direction, whereas for CrO_2 the platelets are aligned along the [001] direction. The aspect ratio of the platelets appears to be controlled by the strain anisotropy, with the CrO_2 films exhibiting platelets with smaller aspect ratio because of the lower anisotropy. In addition, the average grain size and the root mean square (RMS) roughness scale linearly with thickness in both cases (see Fig. 1), with the ratio of the RMS roughness to the thickness being ~5.6% and 3.2% for the RuO_2 and CrO_2 films, respectively. We have previously reported on the growth of strain-free CrO_2 on TiO_2 substrates

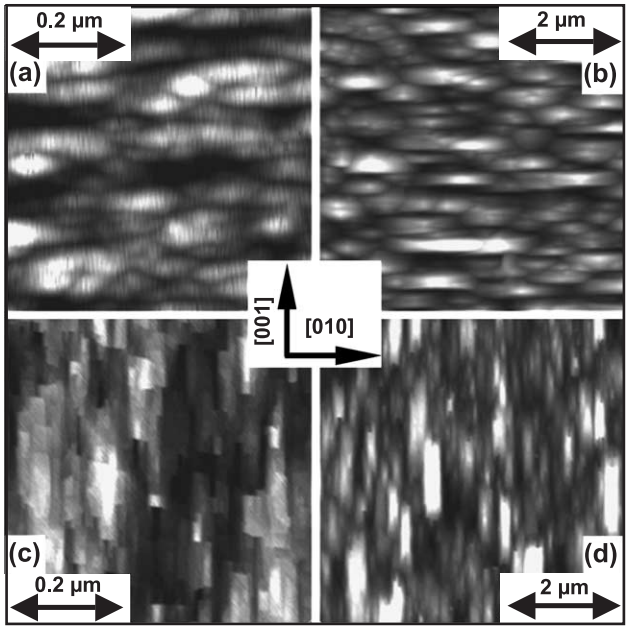

Fig. 1. AFM images of thin and thick RuO_2 (a, b) and CrO_2 (c, d) films. The thickness and accompanying RMS roughness of the films are as follows: (a) 10 nm RuO_2, 1.0 nm; (b) 350 nm RuO_2, 20.5 nm; (c) 35 nm CrO_2, 0.92 nm; and (d) 220 nm CrO_2, 4.6 nm. Note the different length scales for the grains of the thin and thick films.

[19], which do not undergo the HF treatment, where the grains are observed to grow as square-like platelets. This is to be expected based on the present observation of the influence of strain on the growth morphology.

The normal θ–2θ X-ray scans in the vicinity of the (200) peaks of the film and the substrate, for RuO_2 and CrO_2 films of different thicknesses, are shown in Fig. 2(a) and (b), respectively. In the case of the latter, because of the anisotropic in-plane tensile strain imposed on the film, there is a consequent shrinkage of the a-axis lattice parameter perpendicular to the substrate. This is evident from the shift in the CrO_2 film peak to higher angles with decreasing thickness (Fig. 2(b)) as they are more coherently strained. The RuO_2 films experience a combination of compressive and tensile strain in the plane. However, the compressive component dominates because of the larger mismatch in the [001] direction. The result is an expansion in the out-of-plane direction and a shift of the Bragg peak position to lower angles, as seen in Fig. 2(a). The rocking curve full width at half maximum of the (200) peaks for both RuO_2 and CrO_2 are quite narrow, being in the range of 0.1–0.3°. The epitaxy of both films is confirmed from φ-scan measurements of the off-axis (220) peaks, where the expected two-fold symmetry is observed. It should be noted that the lattice parameter of RuO_2 films along [100], as calculated from the position of the (200) peak for thick films, is about 0.9% lower than the bulk value. We do not have an explanation for this behavior, but believe that it is possibly caused by some oxygen deficiency in the as-deposited RuO_2 films or by the strain induced deformation of the RuO_6 octahedrons.

The films have been patterned using standard photolithographic techniques for resistivity measurements along the [010] and [001] directions by the four-probe method. A log–log plot of the resistivity, ρ, as a function of temperature (T) for epitaxial RuO_2 and CrO_2 films on (100) TiO_2 substrates is shown in Fig. 3. The films that have been measured are relatively thick, in the range of 200–400 nm, for which significant strain-effects are not likely. Both materials exhibit the expected metallic behavior, with a

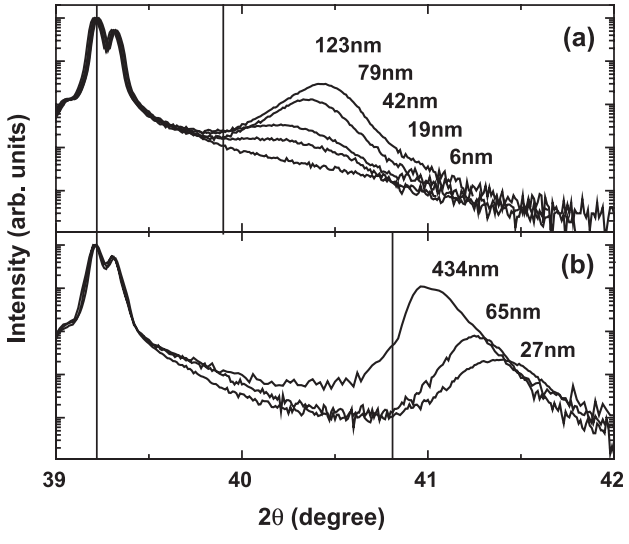

Fig. 2. Normal θ–2θ X-ray diffraction patterns for (a) RuO_2 and (b) CrO_2 films of different thicknesses deposited on (100) TiO_2 substrates. The vertical lines mark the expected position of the (200) peak for the substrate and the respective films from reported bulk measurements.

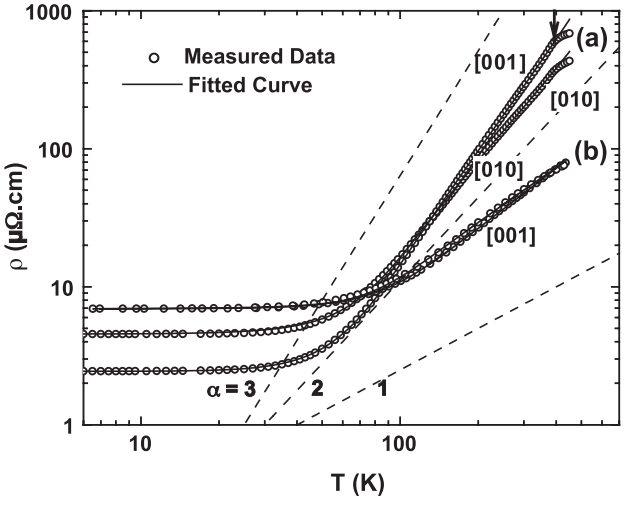

Fig. 3. Plot (log–log) of the resistivity as a function of temperature for (a) 400 nm CrO_2 and (b) 120 nm RuO_2 films along the [010] and [001] directions. A change in slope is observed at T_c for CrO_2 and is marked with an arrow. The solid curves are fits to the experimental data as described in the text. For the purpose of visualization, the T, T^2 and T^3 dependences (α=1, 2 and 3) of ρ versus T are shown as dashed lines that are arbitrarily normalized at 30 K.

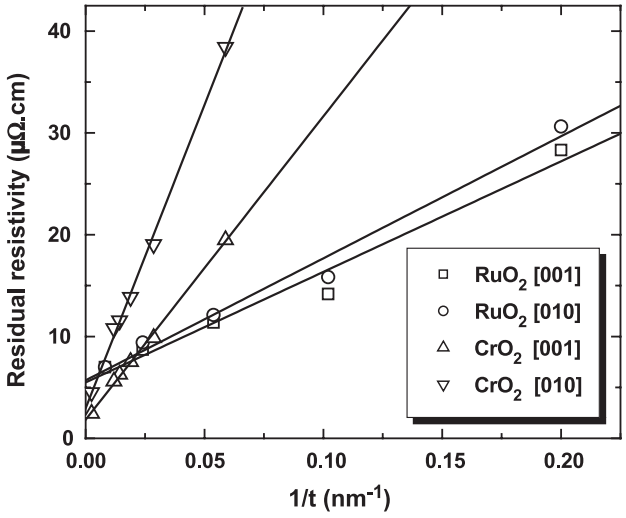

Fig. 4. Plot of the residual resistivity (at 7 K) versus the inverse of the film thickness, ($1/t$), for RuO_2 and CrO_2 films along [010] and [001].

decrease in resistivity as the temperature is lowered. The $\rho(T)$ plot for CrO_2 also shows a slight change in the slope at the Curie temperature (T_c) of 390 K [9]. Measurements on bulk single crystals have shown that, while the resistivity of RuO_2 is isotropic in the plane [20], CrO_2 displays a large difference in the two directions [21]. Our results are qualitatively consistent, except that we do observe a small anisotropy even for RuO_2 that could possibly be related to the effect of some residual strain. It is worth noting that, while both materials are goods conductors at low temperatures, CrO_2 is a rather poor metal at elevated temperatures—exhibiting a room-temperature resistivity almost an order of magnitude higher than that of RuO_2.

The $\rho(T)$ data for both the films along the two in-plane axes directions can be fitted well with a constant residual resistivity term, ρ_0, plus other temperature dependent terms:

$$\rho(T) = \rho_0 + \rho_1\left(\frac{T}{\theta}\right)^5 \int_0^{\theta/T} \frac{x^5 \mathrm{d}x}{(\mathrm{e}^x - 1)(1 - \mathrm{e}^{-x})} + \rho_2 T^2 + \rho_3 T^3 \quad (1)$$

The term with the ρ_1 coefficient is the standard Bloch-Grüneisen (BG) contribution from electron–phonon scatterings. A T^2 contribution is expected from electron–electron scattering, and also from one-magnon scattering in the case of normal ferromagnetic metals [22]. The T^3 term is unique to half-metals, such as CrO_2, that has recently been proposed by Furukawa based on the argument that unconventional one-magnon scattering process can contribute in a half-metal if the non-rigid band behavior of the minority band due to spin fluctuations at finite temperatures is considered [23,24]. If single-magnon scattering is strictly disallowed, then two-magnon scattering processes in half-metals would result in a $T^{4.5}$ dependence [25]. However, its contribution would be negligible and difficult to detect in the presence of an unconventional one-magnon scattering contribution. Since RuO_2 is non-magnetic, no contribution to its resistivity from any of these two terms is expected. It is seen from the fitting in Fig. 4 that the overall exponent for CrO_2 from T_c to about 40–50 K is between 2 and 3, while that for RuO_2 in the range of 100–300 K is between 1 and 2.

From the fit to the resistivity curves, we have determined the Debye temperature, θ_D, of CrO_2 to be about 670 K, while that for RuO_2 is about 580 K. Both these values are lower than the θ_D of ~775 K for rutile-TiO_2 [26] and are to be expected based on the relative mass of the cations.

We have also measured the resistivity of CrO_2 and RuO_2 films as a function of thickness, with thicknesses down to 17 and 5 nm, respectively. They all display metallic behavior, even down to the thinnest films, with no appreciable change in the functional form of $\rho(T)$. The most prominent effect of the thickness variation is the change in the residual resistivity at low temperatures. Fig. 4 shows a plot of the residual resistivity as a function of inverse thickness ($1/t$) from measurements of RuO_2 and CrO_2 films in the two in-plane directions. From the observed linear dependence, it is clear that surface scattering contributes a significant portion to the resistivity with decreasing thickness as the electron mean free path becomes comparable or larger than the film thickness. The surface scattering appears to be stronger in the case of CrO_2 as suggested by the steeper slope, with some difference in the two directions suggesting added influence of strain.

In summary, we have deposited high-quality epitaxial RuO_2 films on (100) TiO_2 substrates using CVD and the process is fully compatible with the deposition of CrO_2 films. By comparing the properties of these two series of films, we believe that it is feasible to fabricate epitaxial $CrO_2/RuO_2/CrO_2$ heterostructures and investigate their interfacial magnetic anisotropy and spin transport properties.

Acknowledgements

This work was supported by NSF DMR-0306711 and NSF DMR-0080031.

References

[1] G.V. Samsonov, The Oxide Handbook, IFI/Plenum, New York, 1982.
[2] E. Kolawa, F.C.T. So, E.T.-S. Pan, M.-A. Nicolet, Appl. Phys. Lett. 50 (1987) 854.
[3] L. Krusin-Elbaum, M. Wittmer, D.S. Yee, Appl. Phys. Lett. 50 (1987) 1879.
[4] A. Belkind, Z. Orban, J.L. Vossen, J.A. Wollam, Thin Solid Films 50 (1992) 242.
[5] H.N. Al-Shareef, K.R. Bellur, A.I. Kingon, O. Auciello, Appl. Phys. Lett. 66 (1995) 239.
[6] H.C. Lee, W.J. Lee, Jpn. J. Appl. Phys. 1 (40) (2001) 6566.

[7] Y. Kim, S.-C. Ha, K.-C. Jeong, H. Hong, J.-S. Roh, H.K. Yoon, Integr. Ferroelectr. 36 (2001) 285.
[8] Y. Ji, G.J. Strijkers, F.Y. Yang, C.L. Chien, J.M. Byers, A. Anguelouch, G. Xiao, A. Gupta, Phys. Rev. Lett. 86 (2001) 5585.
[9] A. Gupta, X.W. Li, G. Xiao, J. Appl. Phys. 87 (2000) 6073.
[10] S.M. Watts, S. Wirth, S. von Molnar, A. Barry, J.M.D. Coey, Phys. Rev., B 61 (2000) 9621.
[11] A. Anguelouch, A. Gupta, G. Xiao, D.W. Abraham, Y. Ji, S. Ingvarsson, C.L. Chien, Phys. Rev., B 64 (2001) 180408R.
[12] R.H. Cheng, Z.Y. Liu, X. Bo, S. Adenwalla, L. Yuan, S.H. Liou, P.A. Dowben, Mater. Lett. 56 (2002) 295.
[13] Y.-H. Lai, Y.-L. Chen, Y. Chi, C.-S. Liu, A.J. Carty, S.-M. Peng, G.-H. Lee, J. Mater. Chem. 13 (2003) 1999.
[14] G.A. Rizzi, A. Magrin, G. Granozzi, Surf. Sci. 443 (1999) 277.
[15] P. Lu, S. He, F.X. Li, Q.X. Jia, Thin Solid Films 340 (1999) 140.
[16] F. Fröhlich, D. Machajdík, V. Cambel, I. Kostič, S. Pignard, J. Cryst. Growth 235 (2002) 377.
[17] A.M. Bratkovsky, Phys. Rev., B 56 (1997) 2344.
[18] J.M. Lee, J.C. Shin, C.S. Hwang, H.J. Kim, C.-G. Suk, J. Vac. Sci. Technol., A 16 (1998) 2768.
[19] X.W. Li, A. Gupta, G. Xiao, Appl. Phys. Lett. 75 (1999) 713.
[20] W.D. Ryden, A.W. Lawson, C.C. Sartain, Phys. Lett. 26A (1968) 209.
[21] D.S. Rodbell, J.M. Lommel, R.C. DeVries, J. Phys. Soc. Jpn. 21 (1966) 2430.
[22] P.L. Rossiter, The Electrical Resistivity of Metals and Alloys, Cambridge University Press, New York, 1991.
[23] N. Furukawa, J. Phys. Soc. Jpn. 69 (2000) 1954.
[24] T. Akimoto, Y. Morimoto, A. Nakamura, N. Furukawa, Phys. Rev. Lett. 85 (2000) 3914.
[25] N. Kubo, N. Ohata, J. Phys. Soc. Jpn. 33 (1972) 21.
[26] T.R. Sandin, P.H. Keesom, Phys. Rev. 177 (1969) 1370.